Batteries & Supercaps

Research Article
doi.org/10.1002/batt.202100359

Chemistry Europe
European Chemical Societies Publishing

www.batteries-supercaps.org

Special Collection

Full-Range Redox Mediation on Sulfur Redox Kinetics for High-Performance Lithium-Sulfur Batteries

Yan-Qi Peng[+],[a, b] Meng Zhao[+],[a, b] Zi-Xian Chen,[a, b] Qian Cheng,[a, b] Yiran Liu,[a, b] Chang-Xin Zhao,[c] Xinzhi Ma,[d] Bo-Quan Li,*[a, b] Cheng-Meng Chen,[e] Jia-Qi Huang,[a, b] and Qiang Zhang*[c]

Lithium-sulfur (Li–S) battery is considered as a promising energy storage system because of its high theoretical energy density of 2600 Wh kg^{-1}, whose practical performance is limited by the sluggish sulfur redox kinetics. Homogeneous redox mediators (RMs) are effective promotors to propel the sulfur redox kinetics. However, most of the RMs only focus on a single reaction process. Herein, a strategy of mixed redox mediators (mixed-RM) is proposed for full-range redox mediation on the sulfur redox kinetics in working Li–S batteries. Concretely, one of the mixed-RM mainly mediates the liquid-solid reduction from polysulfides (LiPSs) to Li_2S during discharge, while the other aims to promote the solid-liquid conversion from Li_2S to LiPSs and the liquid-solid conversion from LiPSs to S_8 during charge. Consequently, 2.5 Ah Li–S pouch cells with the mixed-RM achieve an actual initial energy density of 354 Wh kg^{-1} alongside stable 20 cycles. This work provides an effective strategy on promoting the sulfur redox kinetics for high-energy-density Li–S batteries and inspires rational combination of novel functional molecules for practical energy storage systems.

Introduction

Developing high-efficiency energy storage techniques is of great importance for massive application of renewable energy sources dealing with the global concerns on energy crisis.[1] Lithium-ion batteries (LIBs) occupy the mainstream commercial position of secondary batteries.[2] However, the limited theoretical specific capacity of the cathode materials of LIBs cannot satisfy the growing demand for high-energy-density secondary batteries beyond 400 Wh kg^{-1}.[3] Lithium-sulfur (Li–S) batteries have attracted more and more attention due to the ultrahigh theoretical energy density up to 2600 Wh kg^{-1}.[4] Besides, the cathode material, sulfur, is naturally abundant and environmentally friendly to afford additional competitive superiority.[5] Therefore, Li–S batteries are highly considered as a promising next-generation secondary battery system to realize practical high energy density beyond the current LIBs.[6]

The sulfur cathode generally undergoes multi-electron and multi-phase redox reactions which are highly sluggish in kinetics.[7] During the discharge process, solid sulfur (S_8) is reduced to dissolved polysulfides (LiPSs) and further reduced to solid lithium sulfide (Li_2S), and the above processes reverse during charge from solid Li_2S oxidized to dissolved LiPSs and further oxidized to solid S_8.[8] These complex sulfur redox reactions with retarded kinetics lead to poor rate response and low discharge capacity especially under practical working conditions with high sulfur loading and lean electrolyte volume.[9] To address the above kinetic challenges, heterogeneous kinetic promoters have been widely investigated and introduced as sulfur hosts or interlayer materials[10] including carbon materials,[11] metals,[12] and metal compounds.[13] These heterogeneous kinetic promoters regulate the polysulfide redox kinetics through surface electrocatalysis and are therefore highly dependent on the conductive surface of the cathode.[14] Once the conductive surface is covered by insulating Li_2S or S_8, the heterogeneous kinetic promoters will be no longer exposed to the sulfur species and their promotion effects will be severely hindered.[15] Moreover, the above

[a] Y.-Q. Peng,[+] M. Zhao,[+] Z.-X. Chen, Q. Cheng, Y. Liu, Dr. B.-Q. Li, Prof. J.-Q. Huang
School of Materials Science and Engineering
Beijing Institute of Technology
Beijing 100081, China
[b] Y.-Q. Peng,[+] M. Zhao,[+] Z.-X. Chen, Q. Cheng, Y. Liu, Dr. B.-Q. Li, Prof. J.-Q. Huang
Advanced Research Institute of Multidisciplinary Science
Beijing Institute of Technology
Beijing 100081, China
E-mail: libq@bit.edu.cn
[c] C.-X. Zhao, Prof. Q. Zhang
Beijing Key Laboratory of Green Chemical Reaction Engineering and Technology
Department of Chemical Engineering
Tsinghua University
Beijing 100084, China
E-mail: zhang-qiang@mails.tsinghua.edu.cn
[d] Prof. X. Ma
Key Laboratory for Photonic and Electronic Bandgap Materials, Ministry of Education
School of Physics and Electronic Engineering
Harbin Normal University
Harbin 150025, China
[e] Prof. C.-M. Chen
Key Laboratory of Carbon Materials
Institute of Coal Chemistry, Chinese Academy of Sciences
Taiyuan 030001, China
[+] These authors contributed equally to this work.

Supporting information for this article is available on the WWW under https://doi.org/10.1002/batt.202100359

Special Collection An invited contribution to a Special Collection dedicated to Lithium-Sulfur Batteries

Research Article
doi.org/10.1002/batt.202100359
Chemistry Europe
European Chemical Societies Publishing

surface covered issue will be deteriorated under high-sulfur-loading and lean-electrolyte working conditions.[16]

Homogeneous redox mediation constitutes another promising approach to promoting the sulfur redox kinetics.[17] Generally, redox mediators (RMs) are soluble in electrolyte and possess faster redox kinetics than the sulfur species.[18] The RMs firstly chemically react with specific sulfur species in electrolyte and then electrochemically recover on electrode.[17c,19] The RMs serve as electron carriers between the sulfur species and the electrode, constructing another pathway for the targeted sulfur redox reactions in parallel with the electrochemical processes.[20] The introduction of RMs relieves the dependence on conductive surface and addresses the surface covered issue causing by Li_2S and S_8.[21] Moreover, the RMs with intrinsically faster redox kinetics accelerate the overall sulfur redox kinetics by affording the redox mediation by-pass to endow promoted battery performances. Huang and co-workers presented the concept through the introduction of a small molecule, cobaltocene, as the RM.[22] The cobaltocene RM effectively improved the deposition rate and dimension of Li_2S during discharge with promoted battery performances. Similarly, a quinone-based RM was proposed to effectively reduce the initial oxidation barrier of bulk Li_2S following the redox mediation principles.[23] In addition, supramolecular polymer perylene bisimide was proved to facilitate the oxidation of Li_2S_8 with higher sulfur utilization and high-rate performances.[24] The development of new RMs creates opportunities for improving a targeted sulfur redox reaction. Nevertheless, full-range mediation on the multistep sulfur redox reactions is still insufficient that one RM can only promote a specific process.[25] New design strategies for full-range mediation are therefore highly critical for the overall kinetic promotion of the sulfur redox reactions and realizing practical high-energy-density Li–S batteries.[26]

Herein, a strategy of mixed redox mediators (mixed-RM) is proposed for full-range mediation on the sulfur redox kinetics of working Li–S batteries (Figure 1). Two RMs are selected to constitute the mixed-RM to comprehensively mediate different conversion processes. Specifically, cobaltocene ($CoCp_2$) functions as a discharge RM (d-RM) to mediate the liquid-solid conversion from LiPSs to Li_2S (Reaction I in Figure 1). Meanwhile, 1,4-naphthoquinone (NQ) is chosen as a charge RM (c-RM) for mediating the solid-liquid conversion from Li_2S to LiPSs (Reaction II in Figure 1) and the liquid-solid conversion from LiPSs to S_8 (Reaction III in Figure 1). Integrating the characteristics of the two RMs, the mixed-RM promotes the sulfur redox kinetics in full range and increases the deposition mode of the solid products from two-dimensional (2D) to three-dimensional (3D). Consequently, the mixed-RM endows improved battery performances under practical working conditions by affording a specific capacity of 734 $mAh\,g^{-1}$ at 0.3 C with high sulfur loading of 4.0 $mg_S\,cm^{-2}$ and low electrolyte to sulfur (E/S) ratio of 5 $\mu L\,mg_S^{-1}$. More importantly, 2.5 Ah Li–S pouch cells with the mixed-RM achieve a high actual energy density of 354 $Wh\,kg^{-1}$ and stable 20 cycles. This work provides an effective strategy for full-range promotion on the sulfur redox kinetics and construction of practical high-energy-density Li–S batteries.

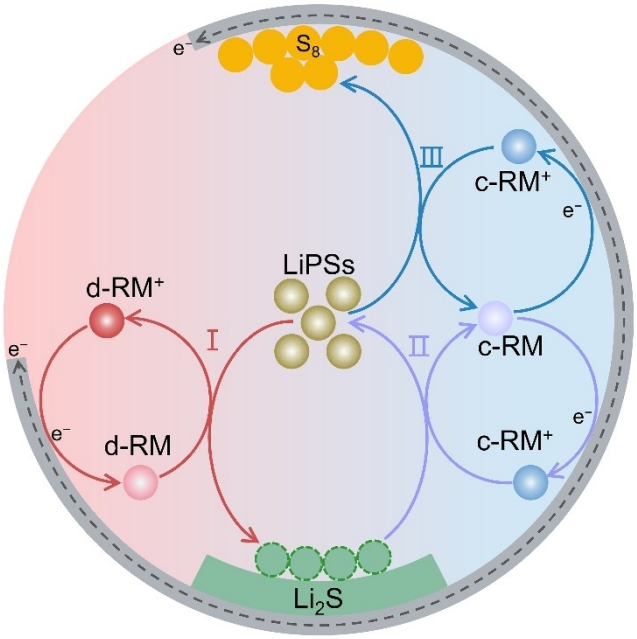

Figure 1. Schematic illustration of the reaction pathway of Li–S batteries mediated by the mixed-RM. The d-RM promotes the reduction kinetics from LiPSs to Li_2S. The c-RM facilitates the oxidization processes from Li_2S to LiPSs and then to S_8.

Results and Discussion

The working potentials of the RMs versus the Li metal anode were firstly evaluated by cyclic voltammetry (CV) to determine the targeted redox mediation process of each RM (Figure 2a). The blank sulfur species presented typical redox behaviors with two cathodic peaks at 2.33 and 2.03 V corresponding to the reduction processes from S_8 to LiPSs and from LiPSs to Li_2S, and two anodic peaks at 2.34 and 2.41 V corresponding to the oxidation processes from Li_2S to LiPSs and from LiPSs to S_8. As expected, the d-RM exhibited a reduction potential of 1.98 V, 50 mV more negative than the reduction of Li_2S. Therefore, the d-RM in the reduced state can chemically reduce LiPSs to Li_2S for redox mediation on the above liquid-solid conversion. On the other hand, the c-RM showed two oxidation peaks at 2.48 and 2.69 V, both higher than the highest oxidation peak of LiPSs. Therefore, the c-RM is capable to oxidize Li_2S and LiPSs to redox mediate the phase conversion processes during charge. In addition, the mixed-RM consisting of the d-RM and the c-RM combined their individual redox potentials with no interference between the two RMs (Figure S1). Based on the above discussion, the mixed-RM is supposed to mediate three processes towards the liquid-solid deposition of LiPSs to Li_2S by the d-RM (reaction I), the solid-liquid dissolution of Li_2S to LiPSs by the c-RM (reaction II), and the liquid-solid deposition of LiPSs to S_8 by the c-RM as well (reaction III) following the redox mediation principles (Figure 2b).

Research Article
doi.org/10.1002/batt.202100359
Chemistry Europe
European Chemical Societies Publishing

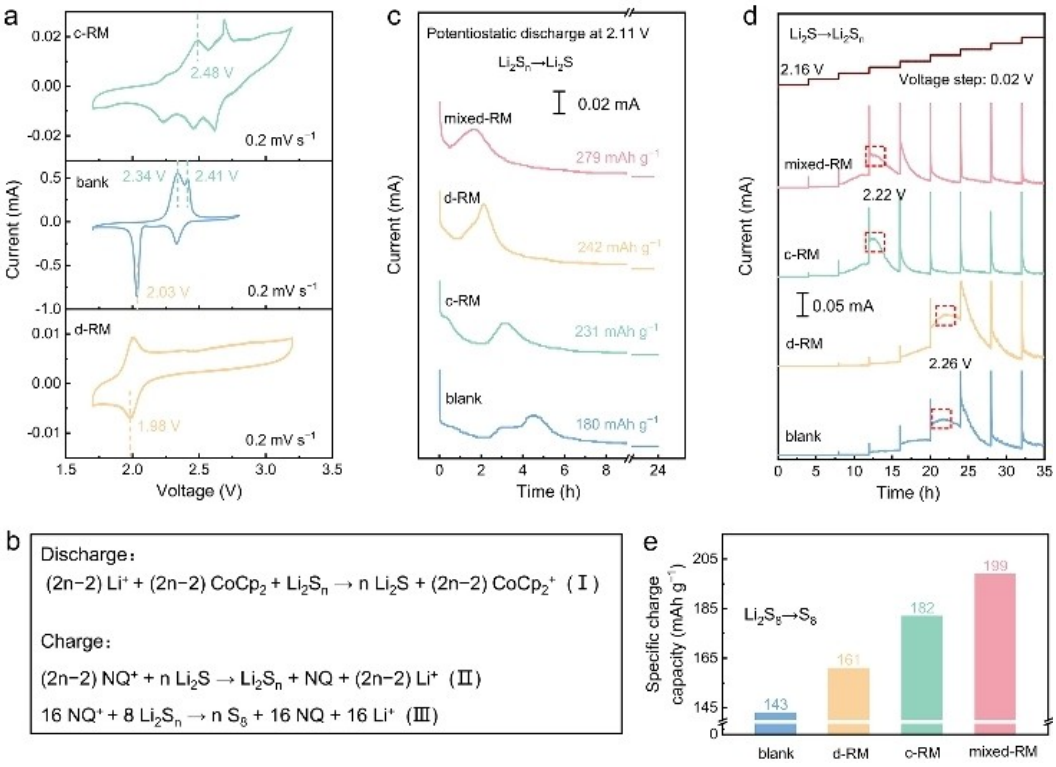

Figure 2. Evaluation of the mixed-RM on the sulfur redox kinetics. a) CV profiles of Li|Li_2S_8, Li|$CoCp_2$, and Li|NQ cells. b) Chemical reactions of d-RM and c-RM with LiPSs during discharge or charge. c) Chronoamperometry curves of Li_2S_8 catholyte discharged at 2.11 V with different RMs. d) PITT measurements of Li|Li_2S cells with different RMs. e) The specific charge capacity of Li|Li_2S_8 cells with different RMs.

To evaluate the liquid-solid conversion kinetics from LiPSs to Li_2S, Li|Li_2S_8 cells with different RMs were assembled and potentiostatically discharged at 2.11 V (Figure 2c).[27] The cells without RMs exhibited a nucleation current peak after about 4.5 h with a deposition capacity of 180 mAh g^{-1}. By contrast, the nucleation peaks of the cells with either d-RM or c-RM appeared 2.4 or 1.4 h earlier than the blank cells with higher deposition capacity of 242 and 231 mAh g^{-1}, respectively. Obviously, the mediation superiority for Li_2S deposition is in favor of the d-RM with earlier peak time and higher deposition capacity than the c-RM. Besides, the cell with the mixed-RM inherited the mediation advantages of the d-RM and provided the earliest peak time of 1.6 h and the highest deposition capacity of 279 mAh g^{-1}, implying that the mediation of the mixed-RM sufficiently promotes the deposition rate and the deposition capability of the liquid-solid sulfur conversion process.

To evaluate the solid-liquid conversion kinetics from Li_2S to LiPSs during the charge process, Li|Li_2S_8 cells were pre-discharged to obtain Li|Li_2S cells for conducting the potentiostatic intermittent titration technique (PITT) tests (Figure 2d). The fully discharged Li|Li_2S cells were charged from 2.16 V to 2.40 V with a voltage step of 20 mV and potentiostatically held for 4.0 h at each voltage step. The dissolution of Li_2S will contribute a current peak according to previous reports,[15] and the potential at which the current peak presents the kinetics for Li_2S oxidation. Li_2S in both the blank cell and the d-RM cell was oxidized at 2.26 V. In comparison, due to the redox mediation effect for Li_2S oxidization, the cell with the c-RM exhibited a current peak at 2.22 V, 40 mV lower than the blank and the d-RM cells. The mixed-RM inherited the advantage of the c-RM and provided lower Li_2S oxidization potential of 2.22 V. The charging PITT results prove that the c-RM endows the mixed-RM with the redox mediation capability to reduce the Li_2S oxidation overpotential and facilitate the solid-liquid conversion kinetics.

Previous researches have demonstrated that there are lots of LiPSs remaining in electrolyte when the Li–S batteries are fully charged, leading to rapid loss of capacity during cycling.[28] Thus, thorough oxidization from LiPSs to S_8 is critical for high-energy-density Li–S batteries. To evaluate the influence of the mixed-RM on the liquid-solid conversion from LiPSs to S_8, Li|Li_2S_8 cells were galvanostatically charged to 2.8 V and the charge capacity was selected as the indicator (Figures 2e and S2). The cells without RM only provided a charge capacity of 143 mAh g^{-1}, while the cells with the d-RM or the c-RM afforded 161 and 182 mAh g^{-1}, respectively. The higher charge capacity of c-RM is largely due to its suitable working potential for oxidizing from LiPSs to S_8. In addition, the cells with the mixed-RM provided the highest charge capacity of 199 mAh g^{-1}, nearly 40% higher than the blank cells. It shall be noted that some of the RMs are electrochemically active and can contribute to battery capacity.[26] To address this concern, cells with d-RM, c-RM, or mixed-RM as active materials were assembled and galvanostatically cycled. The above cells provided specific capacity lower than 5 mAh g^{-1} (Figure S3).

Research Article
doi.org/10.1002/batt.202100359
Chemistry Europe
European Chemical Societies Publishing

Thus, the charge capacity promotion rendered by the RMs is mainly attributed to the strengthened sulfur redox kinetics. Overall, the mixed-RM apparently promotes the redox kinetics of the complex multi-phase sulfur conversion reductions regarding the reduction from LiPSs to Li_2S, the oxidization from Li_2S to LiPSs, and the oxidization from LiPSs to S_8. Full-range redox mediation is realized by using the mixed-RM in Li–S batteries.

To further characterize the effects of the mixed-RM on the deposition behaviors of the solid deposits in Li–S cells, ex-situ morphology characterization was carried out at different depths of discharge or charge using scanning electron microscopy (SEM) (Figure 3). The Li | Li_2S_8 cells with or without the mixed-RM were assembled for galvanostatic discharging (Figure 3a). When the discharge capacity reached 0.1 mAh (Figure $3b_1$), thin films were deposited on the surface of the carbon paper (CP) in the blank cells without RMs compared with the clean CP (Figure S4). With increased discharge depths (Figure $3b_2$), the surface of the CP was gradually covered by 2D flocculent deposits and finally completely covered by insulating deposits (Figure $3b_3$), leading to the premature discharge termination to the 1.7 V cut-off voltage. In contrast, small particles were deposited on the CP at the initial nucleation stage of Li_2S in the cells with the mixed-RM (Figure $3c_1$). In the following discharge process, the particles became dense and grew larger (Figure $3c_2$ and c_3). Evidently, the deposition mode of Li_2S transferred from 2D to 3D under the mediation of the mixed-RM, which is conducive to higher discharge capacity under limited conductive surfaces.

Similarly, the deposition morphology of solid S_8 was studied through galvanostatic charging (Figure 3d). For the cells without the mixed-RM, several deposits appeared locally on the surface of the CP when the charging capacity reached 0.01 mAh (Figure $3e_1$). The deposits gradually grew denser and aggregated together to form a membranous cover on the CP surface when the capacity reached 0.05 mAh (Figure $3e_2$), and finally the deposits formed a thick and dense 2D film coated on the CP when the cell was charged to 2.8 V (Figure $3e_3$). In comparison, the mixed-RM mediated cells exhibited fusiform-shaped S_8 deposition at the initial stage of charging (Figure $3f_1$). When the cells were charged to 0.05 mAh, the fusiform deposits contacted and agglomerated into flower-like clusters (Figure $3f_2$). The CP surface was finally tightly covered by lots of the flower-like clusters when charged to 2.8 V (Figure $3f_3$). The morphology during charge illustrates that the mixed-RM effectively modulates the deposition mode of S_8 transferred from 2D to 3D as well and is in favor of higher charge capacity to improve the conversion from LiPSs to S_8.

The above model experiments and ex-situ morphology characterization have confirmed the advantages of the mixed-RM for full-range sulfur redox kinetics promotion. To confirm the effect of the mixed-RM in working Li–S batteries, Li–S coin cells with sulfur loading of 1.1 $mg_S\ cm^{-2}$ were assembled and evaluated. The mixed-RM cells exhibited reduced polarization and higher peak currents than the blank cells in the CV profiles

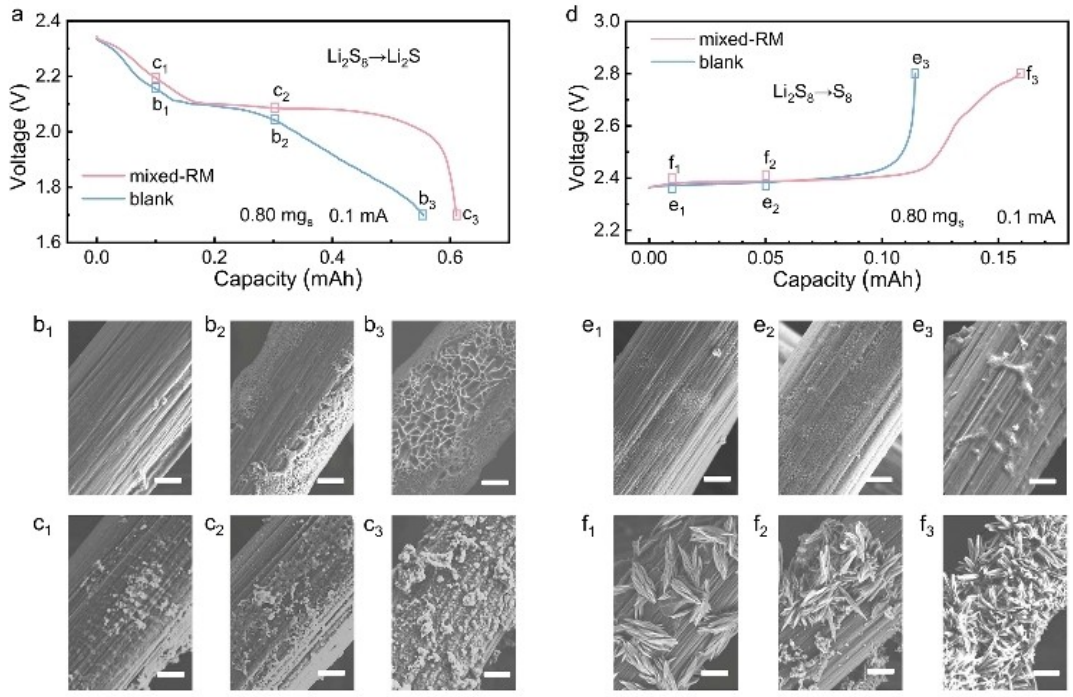

Figure 3. Morphology characterization of Li_2S and S_8 deposits. a) The discharge curves of Li | Li_2S_8 cells with and without the mixed-RM. The cells were terminated at the marked points to characterize the Li_2S deposits on CPs. SEM images of Li_2S deposits on CPs at different depth of discharge b_1–b_3) without the mixed-RM and c_1–c_3) with the mixed-RM. d) The charge curves of Li | Li_2S_8 cells with and without the mixed-RM. The cells were terminated at the marked points to characterize the S_8 deposits on CPs. SEM images of S_8 deposits on CP e_1–e_3) without the mixed-RM and f_1–f_3) with the mixed-RM. The scale bars are 2 μm.

Research Article
doi.org/10.1002/batt.202100359
Chemistry Europe
European Chemical Societies Publishing

(Figure S5). The mixed-RM cells also provided reduced interfacial charge transfer impedance of only 17 Ω, 63 Ω lower than the blank cells (Figure S6). The reduced charge transfer impedance indicates that the mixed-RM greatly improves the redox kinetics of the cells. Accordingly, the Li–S cells with the mixed-RM achieved excellent rate performances with specific capacities of 940, 694, 673, 640, 607, and 580 mAh g^{-1} at 0.1, 0.5, 1, 2, 4, and 6 C (1 C = 1672 mA g^{-1}), respectively, 7%–211% higher than the blank cells (Figure S7a). The charge-discharge curves revealed the origin of the promotion regarding the rate performances (Figure S7b). There was no difference in polarization at a low rate of 0.1 C, but a longer discharge platform for the mixed-RM cells was observed. When the current density increased to 6 C, the second platform of the mixed-RM cells maintained at 1.91 V, while the blank cells almost lost this platform due to the sluggish kinetics, indicating that mixed-RM facilitates the conversion kinetics at high rates.

High sulfur loading and lean electrolyte are the prerequisites to realize high-energy-density Li–S batteries.[6c,28,29] To confirm the feasibility of the mixed-RM in practical Li–S batteries, the areal sulfur loading of the sulfur cathode was increased to 4.0 mg_S cm^{-2}. The cells with the mixed-RM delivered an initial discharge capacity of 791 mAh g^{-1} at 0.3 C and maintained 90% of the initial capacity after 100 cycles (Figure 4a). Although the blank cells could provide similar initial capacity as the mixed-RM cells, the cycling lifespan was severely shortened to only 15 cycles, after which the specific capacity was reduced to about 300 mAh g^{-1}. This phenomenon was mainly due to the sluggish kinetics for Li_2S deposition which made the voltage of the second discharge platform of the blank cells went lower and lower along cycling until the disappearance of this platform (Figures 4b and S8). In contrast, the cells mediated by the mixed-RM maintained the typical dual discharge platforms during the long-term cycling with relative stable discharge specific capacities. It should be noticed that 0.3 C is a relatively high rate for high-sulfur-loading cathodes, where the sulfur redox reactions in the blank cells cannot timely and effectively respond and eventually lead to the failure of the battery. In comparison, the existence of the mixed-RM constructs extra rapid and uninterrupted reaction

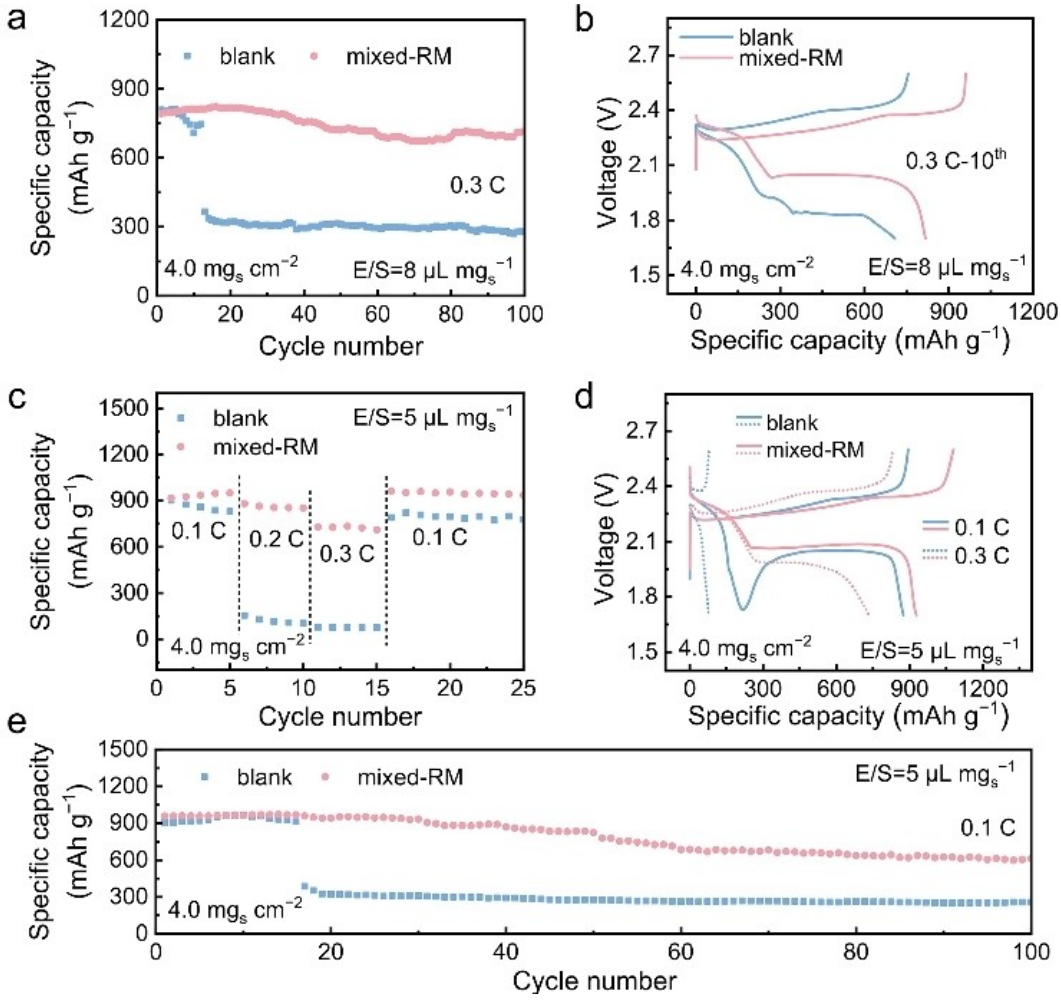

Figure 4. Electrochemical performance of Li–S coin cells. a) Long-term cycling performance at a current density of 0.3 C. b) The 10th galvanostatic discharge-charge profiles at 0.3 C. c) Rate performance of Li–S coin cell under lean-electrolyte conditions. d) Galvanostatic discharge-charge profiles at different current densities corresponding to (c). e) Long-term cycling performance at 0.1 C under lean-electrolyte conditions. The areal sulfur loading in the Li–S coin cells was 4.0 mg_S cm^{-2} and the E/S ratio was 8 μL mg_S^{-1} in a–b) and 5 μL mg_S^{-1} in c–e).

Research Article
doi.org/10.1002/batt.202100359
Chemistry Europe
European Chemical Societies Publishing

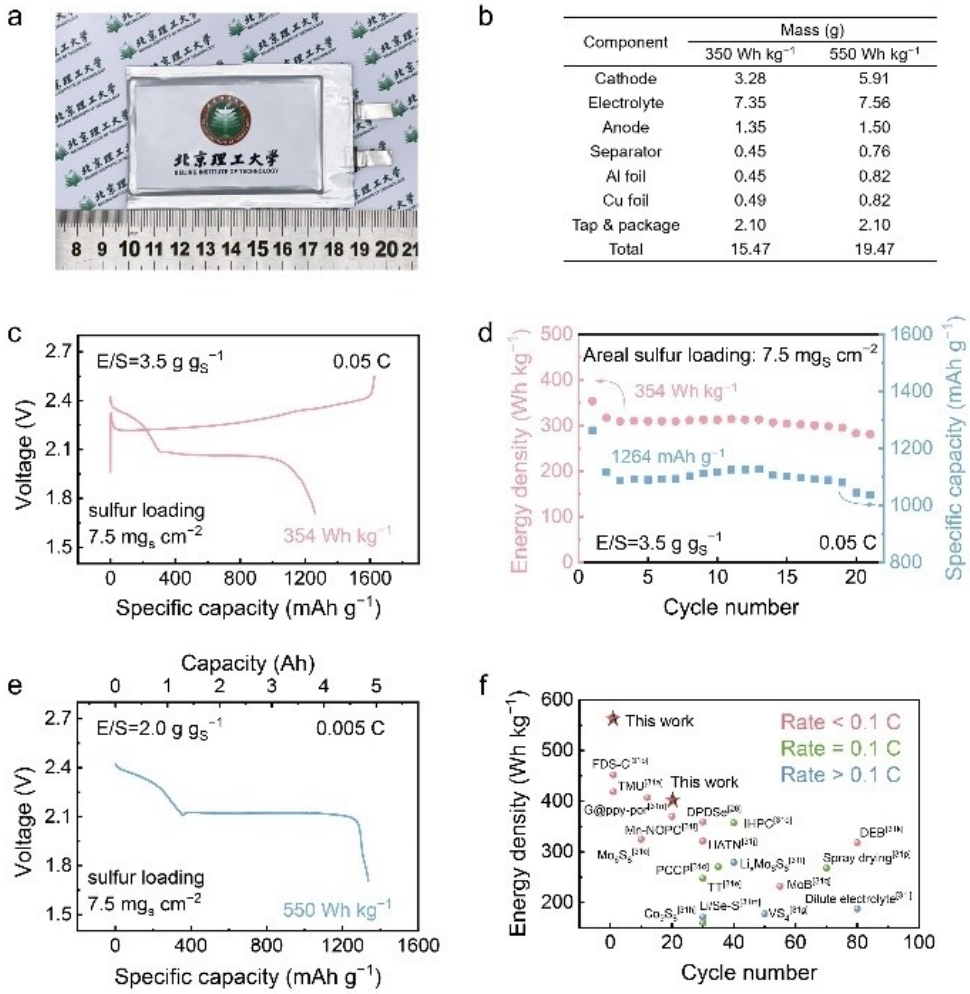

Figure 5. Evaluation on Li–S pouch cells with the mixed-RM. a) Optical photograph of the pouch cell. b) The mass of each component of the Li–S pouch cell with different design energy density. c) Galvanostatic discharge-charge profiles and d) long-term cycling performance of the pouch cell with a design energy density of 350 Wh kg^{-1} at 0.05 C. e) Galvanostatic discharge profile of the pouch cell with a design energy density of 550 Wh kg^{-1} at 0.005 C. f) The performance comparison of Li–S pouch cells with unified mass value of the non-active components.

pathways so that the cells can operate smoothly under high current densities. In addition, although the introduction of mixed-RM inevitably leads to a reduction in Coulombic efficiency due to its own shuttle effect (Figure S9), it shall be noted that the Coulombic efficiency is not directly related to the cyclability of Li anode. The mixed-RM has negligible influence on the cycling stability of Li metal anodes comprehensively proved by the similar Coulombic efficiency values and similar Li deposition morphologies of Li–Ni half cells (Figures S10 and S11).

The amount of electrolyte was further reduced to a low E/S ratio of 5 μL mg_S^{-1} for the evaluation under harsh working conditions (Figure 4c). The mixed-RM cells provided discharge capacities of 937, 863, and 726 mAh g^{-1} on average at 0.1, 0.2, and 0.3 C, respectively. In contrast, the discharge capacity of the blank cells dropped dramatically at 0.2 C. Reduced E/S ratio inevitably increased the LiPS concentration in electrolyte, leading to slow reaction kinetics of the sulfur species.[30] As a result, the discharge curves of the blank cells exhibited a huge nucleation overpotential "pit" before the second discharge platform even under a small current density of 0.1 C, and the second discharge platform was disappeared when the rate increased to 0.3 C (Figure 4d). In contrast, the mixed-RM cells exhibited smooth discharge-charge profiles even at 0.3 C as a result of the full-range redox mediation effects. Long-term cycling under low E/S ratio conditions was conducted to further verify the effect of the mixed-RM (Figure 4e). The mixed-RM cells delivered an initial discharge capacity of 958 mAh g^{-1}, which was 53 mAh g^{-1} higher than that of the blank cells. Along with cycling, the polarization of the blank cells became larger after only 10 cycles with the voltage of the second platform being 1.9 V, and the second platform disappeared after 20 cycles (Figure S12a). Instead, the cells with the mixed-RM exhibited relatively stable voltages of the second platform ranging 2.06–2.08 V. Accordingly, the discharge capacity of the blank cells suddenly decreased to 387 mAh g^{-1} after 17 cycles, while the mixed-RM cells remained stable with a specific capacity of 610 mAh g^{-1} after 100 cycles corresponding to a

specific capacity decay rate of 0.45% per cycle even with a lower Coulombic efficiency of about 82% (Figure S12b). The lifespan of the Li–S cells with high sulfur loading and low E/S ratio was prolonged to more than 3 times due to the full-range redox mediation of the mixed-RM. Compared with previous reports based on different RM strategies, the mixed-RM endows Li–S cells superiority in rate performance and cycling stability under lean-electrolyte conditions (Table S1).

In order to further demonstrate the practical application potential of the mixed-RM, Li–S pouch cells were assembled and evaluated (Figure 5a). The pouch cell with a design energy density of 350 Wh kg^{-1} was assembled with areal sulfur loading of 7.5 $mg_S\,cm^{-2}$ on a single side, an E/S ratio of 3.5 $g\,g_S^{-1}$, and 75 μm-thick Li metal anode. All the components were considered for pouch-cell evaluation including current collectors and packages, and the mass of each component was listed in Figure 5(b). The pouch cell with a design energy density of 350 Wh kg^{-1} provided an initial discharge specific capacity of 1264 mAh g^{-1} with an average discharge voltage of 2.07 V for the second discharge platform (Figure 5c), corresponding to an actual energy density of 354 Wh kg^{-1} based on the actual mass of the cell. Even after 20 cycles, the Li–S pouch cell still delivered a discharge capacity of 1045 mAh g^{-1} corresponding to an energy density of 283 Wh kg^{-1} and an energy density retention rate of 80% although the Coulombic efficiency fluctuated around 80% (Figures 5d and S13). When the E/S ratio was further decreased to 2.0 $g\,g_S^{-1}$ and the thickness of Li metal was controlled as 50 μm, a record-breaking actual energy density of 550 Wh kg^{-1} for Li–S pouch cells was realized with a capacity of 5.0 Ah and smooth discharge voltage at 2.1 V at 0.005 C (Figure 5e and f).[26,31] The high actual energy density and cycling stability of the pouch cells strongly proved the effectiveness of the full-range redox mediation of the mixed-RM on realizing practical high-energy-density Li–S batteries.

Conclusion

In summary, a strategy of mixed-RM is proposed for full-range redox mediation on the sulfur redox kinetics for high-energy-density Li–S batteries. The mixed-RM consisting of a d-RM for the discharge process and a c-RM for the charge process renders significant kinetic promotion toward the liquid-solid conversion from LiPSs to Li_2S and solid-liquid-solid conversion from Li_2S to LiPSs and then to S_8. Accordingly, Li–S coin cells with the mixed-RM provide a discharge capacity of 734 mAh g^{-1} and triple extended lifespan under harsh conditions of high sulfur loading of 4.0 $mg_S\,cm^{-2}$, low E/S ratio of 5 $\mu L\,mg^{-1}$, and high rate of 0.3 C. Moreover, 2.5 Ah Li–S pouch cells with the mixed-RM achieve an actual initial energy density of 354 Wh kg^{-1} and remained 80% of the initial energy density after 20 cycles. The mixed-RM strategy realizes full-range kinetic promotion on the sulfur redox reactions and demonstrates promising potential for the construction of high-performance and high-energy-density Li–S batteries through the combination of novel RM molecules.

Acknowledgements

This work was supported by Natural Scientific Foundation of China (22109007 and 21825501), Beijing Natural Science Foundation (JQ20004), Scientific and Technological Key Project of Shanxi Province (20191102003), National Key Research and Development Program (2021YFB2500300), Beijing Institute of Technology Research Fund Program for Young Scholars, Tsinghua University Initiative Scientific Research Program, and the Open Project Program (PEBM202115) of Key Laboratory for Photonic and Electric Bandgap Materials, Ministry of Education. We thank Dr. Xue-Qiang Zhang, Li-Peng Hou, Yun-Wei Song, Xi-Yao Li, and Chen-Xi Bi for helpful discussion.

Conflict of Interest

The authors declare no conflict of interest.

Data Availability Statement

The data that support the findings of this study are available from the corresponding author upon reasonable request.

Keywords: lithium-sulfur batteries · redox mediation · sulfur redox kinetics · lithium polysulfides · pouch cells

[1] Z. Wei, J. Zhao, H. He, G. Ding, H. Cui, L. Liu, *J. Power Sources* **2021**, *489*, 229462.
[2] a) L. Kong, C. Tang, H. J. Peng, J. Q. Huang, Q. Zhang, *SmartMat* **2020**, *1*, e1007; b) F. Wu, J. Maier, Y. Yu, *Chem. Soc. Rev.* **2020**, *49*, 1569–1614; c) J. Liu, H. Yuan, X. Tao, Y. Liang, S. J. Yang, J. Q. Huang, T. Q. Yuan, M. M. Titirici, Q. Zhang, *EcoMat* **2020**, *2*, e12019.
[3] a) M. Li, J. Lu, Z. Chen, K. Amine, *Adv. Mater.* **2018**, *30*, 1800561; b) E. Fan, L. Li, Z. Wang, J. Lin, Y. Huang, Y. Yao, R. Chen, F. Wu, *Chem. Rev.* **2020**, *120*, 7020–7063.
[4] a) X. Liu, Y. Li, X. Xu, L. Zhou, L. Mai, *J. Energy Chem.* **2021**, *61*, 104–134; b) M. Wu, Y. Li, X. Liu, S. Yang, J. Ma, S. Dou, *SmartMat* **2021**, *2*, 5–11.
[5] A. Rosenman, E. Markevich, G. Salitra, D. Aurbach, A. Garsuch, F. F. Chesneau, *Adv. Energy Mater.* **2015**, *5*, 1500212.
[6] a) Z. W. Seh, Y. Sun, Q. Zhang, Y. Cui, *Chem. Soc. Rev.* **2016**, *45*, 5605–5634; b) A. Manthiram, S.-H. Chung, C. Zu, *Adv. Mater.* **2015**, *27*, 1980–2006; c) S. Yuan, T. Kong, Y. Zhang, P. Dong, Y. Zhang, X. Dong, Y. Wang, Y. Xia, *Angew. Chem. Int. Ed.* **2021**, *60*, 25624–25638; *Angew. Chem.* **2021**, *133*, 25828–25842;d) Y. X. Yao, X. Q. Zhang, B. Q. Li, C. Yan, P. Y. Chen, J. Q. Huang, Q. Zhang, *InfoMat* **2020**, *2*, 379–388.
[7] a) J. He, A. Manthiram, *Energy Storage Mater.* **2019**, *20*, 55–70; b) Y.-W. Song, Y.-Q. Peng, M. Zhao, Y. Lu, J.-N. Liu, B.-Q. Li, Q. Zhang, *Small Sci.* **2021**, *1*, 2100042.
[8] N. Angulakshmi, R. B. Dhanalakshmi, S. Sathya, J.-H. Ahn, A. M. Stephan, *Batteries & Supercaps* **2021**, *4*, 1064–1095.
[9] a) L. Kong, L. Yin, F. Xu, J. Bian, H. Yuan, Z. Lu, Y. Zhao, *J. Energy Chem.* **2021**, *55*, 80–91; b) L. Mao, H. Xie, F. Wang, J. Mao, *Batteries & Supercaps* **2021**, doi: 10.1002/batt.202100192.
[10] J. Li, Z. Niu, C. Guo, M. Li, W. Bao, *J. Energy Chem.* **2021**, *54*, 434–451.
[11] a) T. Boenke, P. Härtel, S. Dörfler, T. Abendroth, F. Schwotzer, H. Althues, S. Kaskel, *Batteries & Supercaps* **2021**, *4*, 989–1002; b) R. Lu, M. Cheng, L. Mao, M. Zhang, H. Yuan, K. Amin, C. Yang, Y. Cheng, Y. Meng, Z. Wei, *EcoMat* **2020**, *2*, e12010; c) Z. Zhang, L. L. Kong, S. Liu, G. R. Li, X. P. Gao, *Adv. Energy Mater.* **2017**, *7*, 1602543.
[12] a) C.-Y. Fan, P. Xiao, H.-H. Li, H.-F. Wang, L.-L. Zhang, H.-Z. Sun, X.-L. Wu, H.-M. Xie, J.-P. Zhang, *ACS Appl. Mater. Interfaces* **2015**, *7*, 27959–27967;

b) G. Zhou, H. Tian, Y. Jin, X. Tao, B. Liu, R. Zhang, Z. W. Seh, D. Zhuo, Y. Liu, J. Sun, *Proc. Natl. Acad. Sci. USA* **2017**, *114*, 840–845.
[13] a) Q. Wang, H. Zhao, B. Li, C. Yang, M. Li, Y. Li, P. Han, M. Wu, T. Li, R. Liu, *Chin. Chem. Lett.* **2021**, *32*, 1157–1160; b) J. Y. Hwang, H. M. Kim, S. Shin, Y. K. Sun, *Adv. Funct. Mater.* **2018**, *28*, 1704294; c) R. R. Dharmasena, A. Martinez-Garcia, V. Atla, M. Z. Akram, G. U. Sumanasekera, M. K. Sunkara, *Batteries & Supercaps* **2020**, *3*, 275–283.
[14] a) C. Geng, W. Hua, D. Wang, G. Ling, C. Zhang, Q. H. Yang, *SusMat* **2021**, *1*, 51–65; b) Y. Zhang, P. Zhang, S. Zhang, Z. Wang, N. Li, S. R. P. Silva, G. Shao, *InfoMat* **2021**, *3*, 790–803; c) C. Zha, D. Wu, X. Gu, H. Chen, *J. Energy Chem.* **2021**, *59*, 599–607; d) L. Giebeler, J. Balach, *Mater. Today Commun.* **2021**, *27*, 102323; e) H. Ye, J. Sun, S. Zhang, T. Zhang, Y. Zhao, C. Song, Q. Yao, J. Y. Lee, *Chem. Eng. J.* **2021**, *410*, 128284.
[15] B. Q. Li, L. Kong, C. X. Zhao, Q. Jin, X. Chen, H. J. Peng, J. L. Qin, J. X. Chen, H. Yuan, Q. Zhang, *InfoMat* **2019**, *1*, 533–541.
[16] a) L. Du, H. Wang, M. Yang, L. Liu, Z. Niu, *Small Struct.* **2020**, *1*, 2000047; b) S. Kumar, K. Krishnamoorthy, *Batteries & Supercaps* **2021**, doi: 10.1002/batt.202100229.
[17] a) W. G. Lim, S. Kim, C. Jo, J. Lee, *Angew. Chem. Int. Ed.* **2019**, *58*, 18746–18757; *Angew. Chem.* **2019**, *131*, 18920–18931; b) H. Ye, J. Sun, X. F. Lim, Y. Zhao, J. Y. Lee, *Energy Storage Mater.* **2021**, *38*, 338–343; c) C. X. Zhao, W. J. Chen, M. Zhao, Y. W. Song, J. N. Liu, B. Q. Li, T. Yuan, C. M. Chen, Q. Zhang, J. Q. Huang, *EcoMat* **2021**, *3*, e12066.
[18] X. Q. Zhang, Q. Jin, Y. L. Nan, L. P. Hou, B. Q. Li, X. Chen, Z. H. Jin, X. T. Zhang, J. Q. Huang, Q. Zhang, *Angew. Chem. Int. Ed.* **2021**, *60*, 15503–15509; *Angew. Chem.* **2021**, *133*, 15631–15637.
[19] C.-W. Lee, Q. Pang, S. Ha, L. Cheng, S.-D. Han, K. R. Zavadil, K. G. Gallagher, L. F. Nazar, M. Balasubramanian, *ACS Cent. Sci.* **2017**, *3*, 605–613.
[20] J. Li, L. Yang, S. Yang, J. Y. Lee, *Adv. Energy Mater.* **2015**, *5*, 1501808.
[21] a) S. Meini, R. Elazari, A. Rosenman, A. Garsuch, D. Aurbach, *J. Phys. Chem. Lett.* **2014**, *5*, 915–918; b) L. C. H. Gerber, P. D. Frischmann, F. Y. Fan, S. E. Doris, X. Qu, A. M. Scheuermann, K. Persson, Y.-M. Chiang, B. A. Helms, *Nano Lett.* **2016**, *16*, 549–554.
[22] M. Zhao, H. J. Peng, J. Y. Wei, J. Q. Huang, B. Q. Li, H. Yuan, Q. Zhang, *Small Methods* **2020**, *4*, 1900344.
[23] a) Y. Tsao, M. Lee, E. C. Miller, G. Gao, J. Park, S. Chen, T. Katsumata, H. Tran, L.-W. Wang, M. F. Toney, Y. Cui, Z. Bao, *Joule* **2019**, *3*, 872–884; b) C. Y. Chen, H. J. Peng, T. Z. Hou, P. Y. Zhai, B. Q. Li, C. Tang, W. Zhu, J. Q. Huang, Q. Zhang, *Adv. Mater.* **2017**, *29*, 1606802.
[24] a) P. D. Frischmann, L. C. H. Gerber, S. E. Doris, E. Y. Tsai, F. Y. Fan, X. Qu, A. Jain, K. A. Persson, Y.-M. Chiang, B. A. Helms, *Chem. Mater.* **2015**, *27*, 6765–6770; b) P. D. Frischmann, Y. Hwa, E. J. Cairns, B. A. Helms, *Chem. Mater.* **2016**, *28*, 7414–7421.
[25] Y. Song, W. Cai, L. Kong, J. Cai, Q. Zhang, J. Sun, *Adv. Energy Mater.* **2020**, *10*, 1901075.
[26] M. Zhao, X. Chen, X. Y. Li, B. Q. Li, J. Q. Huang, *Adv. Mater.* **2021**, *33*, 2007298.
[27] M. Zhao, X.-Y. Li, X. Chen, B.-Q. Li, S. Kaskel, Q. Zhang, J.-Q. Huang, *eScience* **2021**, *1*, 44–52.
[28] G. Ye, M. Zhao, L.-P. Hou, W.-J. Chen, X.-Q. Zhang, B.-Q. Li, J.-Q. Huang, *J. Energy Chem.* **2022**, *66*, 24–29.
[29] T. Liu, H. Li, J. Yue, J. Feng, M. Mao, X. Zhu, Y.-s. Hu, H. Li, X. Huang, L. Chen, *Angew. Chem. Int. Ed.* **2021**, *60*, 17547–17555; *Angew. Chem.* **2021**, *133*, 17688–17696.
[30] M. Zhao, B. Q. Li, H. J. Peng, H. Yuan, J. Y. Wei, J. Q. Huang, *Angew. Chem. Int. Ed.* **2020**, *59*, 12636–12652; *Angew. Chem.* **2020**, *132*, 12736–12753.
[31] a) G. Zhang, H. J. Peng, C. Z. Zhao, X. Chen, L. D. Zhao, P. Li, J. Q. Huang, Q. Zhang, *Angew. Chem. Int. Ed.* **2018**, *57*, 16732–16736; *Angew. Chem.* **2018**, *130*, 16974–16978; b) Y. Xie, G. Pan, Q. Jin, X. Qi, T. Wang, W. Li, H. Xu, Y. Zheng, S. Li, L. Qie, Y. Huang, J. Li, *Adv. Sci.* **2020**, *7*, 1903168; c) W. Xue, Z. Shi, L. Suo, C. Wang, Z. Wang, H. Wang, K. P. So, A. Maurano, D. Yu, Y. Chen, L. Qie, Z. Zhu, G. Xu, J. Kong, J. Li, *Nat. Energy* **2019**, *4*, 374–382; d) L. Wang, S. Liu, J. Hu, X. Zhang, X. Li, G. Zhang, Y. Li, C. Zheng, X. Hong, H. Duan, *Nano Res.* **2021**, *14*, 1355–1363; e) C. Weller, S. Thieme, P. Härtel, H. Althues, S. Kaskel, *J. Electrochem. Soc.* **2017**, *164*, A3766–A3771; f) W. Xue, D. Yu, L. Suo, C. Wang, Z. Wang, G. Xu, X. Xiao, M. Ge, M. Ko, Y. Chen, L. Qie, Z. Zhu, A. S. Helal, W.-K. Lee, J. Li, *Matter* **2019**, *1*, 1047–1060; g) L. Luo, J. Li, H. Yaghoobnejad Asl, A. Manthiram, *ACS Energy Lett.* **2020**, *5*, 1177–1185; h) J. He, Y. Chen, A. Manthiram, *Energy Environ. Sci.* **2018**, *11*, 2560–2568; i) M. Zhong, J. Guan, J. Sun, X. Shu, H. Ding, L. Chen, N. Zhou, Z. Xiao, *Energy Storage Mater.* **2021**, *41*, 588–598; j) X. Wang, Y. Yang, C. Lai, R. Li, H. Xu, D. H. S. Tan, K. Zhang, W. Yu, O. Fjeldberg, M. Lin, W. Tang, Y. S. Meng, K. P. Loh, *Angew. Chem. Int. Ed.* **2021**, *60*, 11359–11369; *Angew. Chem.* **2021**, *133*, 11460–11470; k) C. Zhao, G. L. Xu, Z. Yu, L. Zhang, I. Hwang, Y. X. Mo, Y. Ren, L. Cheng, C. J. Sun, Y. Ren, X. Zuo, J. T. Li, S. G. Sun, K. Amine, T. Zhao, *Nat. Nanotechnol.* **2021**, *16*, 166–173; l) F. Wu, F. Chu, G. A. Ferrero, M. Sevilla, A. B. Fuertes, O. Borodin, Y. Yu, G. Yushin, *Nano Lett.* **2020**, *20*, 5391–5399; m) C. Zhao, G. L. Xu, T. Zhao, K. Amine, *Angew. Chem. Int. Ed.* **2020**, *59*, 17634–17640; *Angew. Chem.* **2020**, *132*, 17787–17793; n) C. X. Zhao, X. Y. Li, M. Zhao, Z. X. Chen, Y. W. Song, W. J. Chen, J. N. Liu, B. Wang, X. Q. Zhang, C. M. Chen, B. Q. Li, J. Q. Huang, Q. Zhang, *J. Am. Chem. Soc.* **2021**, *143*, 19865–19872; o) G. Xu, D. Yu, D. Zheng, S. Wang, W. Xue, X. E. Cao, H. Zeng, X. Xiao, M. Ge, W. K. Lee, M. Zhu, *iScience* **2020**, *23*, 101576; p) Z. Shi, J. Wei, H. Xu, L. Wang, H. Yue, Z. Cao, H. Dong, Y. Yin, S. Yang, *Chem. Eng. J.* **2020**, *379*, 122353; q) J. He, A. Bhargav, A. Manthiram, *Adv. Mater.* **2020**, *32*, 2004741.

Manuscript received: November 23, 2021
Revised manuscript received: December 15, 2021
Accepted manuscript online: December 17, 2021
Version of record online: December 30, 2021